J. Fluid Mech. (1982), vol. 116, pp. 77–90
Printed in Great Britain

The vortex-shedding process behind two-dimensional bluff bodies

By A. E. PERRY, M. S. CHONG AND T. T. LIM
Department of Mechanical Engineering, University of Melbourne, Parkville, Victoria 3052, Australia

(Received 5 June 1980 and in revised form 26 June 1981)

Using a variety of flow-visualization techniques, the flow behind a circular cylinder has been studied. The results obtained have provided a new insight into the vortex-shedding process. Using time-exposure photography of the motion of aluminium particles, a sequence of instantaneous streamline patterns of the flow behind a cylinder has been obtained. These streamline patterns show that during the starting flow the cavity behind the cylinder is closed. However, once the vortex-shedding process begins, this so-called 'closed' cavity becomes open, and instantaneous 'alleyways' of fluid are formed which penetrate the cavity. In addition, dye experiments also show how layers of dye and hence vorticity are convected into the cavity behind the cylinder, and how they are eventually squeezed out.

1. Introduction

The earliest recorded observation of the phenomenon of vortex shedding can be traced back to the sixteenth century when Leonardo da Vinci made drawings of the surface pattern of the fluid flow past an obstacle (see Popham 1946). It is surprising, but true, that up until now very little has been understood about the formation of vortices that accompany the flow past two- or three-dimensional bluff bodies. The investigation of vortex shedding is important in aerodynamic drag, structural vibration and turbulent mixing.

Over the years, both experimental and theoretical studies have been carried out by various research workers into the nature of vortex shedding. Extensive reviews of this topic have been given by Wille (1960, 1966), Morkovin (1964), Mair & Maull (1971), Berger & Wille (1972), and more recently by Bearman & Graham (1980).

The present authors believe that a deep insight into the mechanism of vortex shedding can be obtained by studying the instantaneous streamline patterns at various phases of the vortex-shedding cycle. Cantwell (1975) made an attempt in this direction when investigating the turbulent wake of a circular cylinder at a Reynolds number of 140000. By using a flying hot-wire technique, and conditionally sampling the data on the basis of phase, he was able to obtain a series of phase-averaged streamline patterns for the far wake for each stage of vortex shedding. However, Cantwell's results provide very little information for the flow in the cavity where vortices are being formed. Using a similar idea, Perry & Watmuff (1981) also made a study of turbulent wakes behind a three-dimensional bluff body. By propelling an air-bearing sled (to which the hot-wire probes were attached) along the centre line of the tunnel, a series of phase-averaged vector fields was obtained which corre-

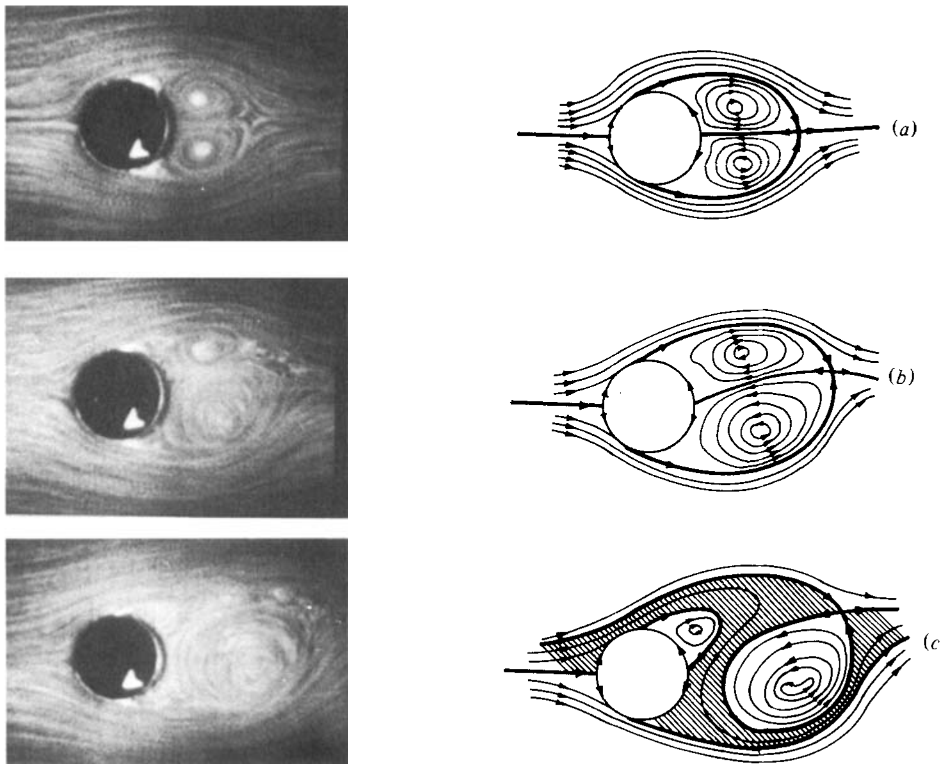

Caption for figures 1 (*a–c*) on p. 79.

sponded to different parts of the vortex-shedding cycle. The results for the far wake were similar to the two-dimensional wakes, but again very little information was obtained in the near wake.

The authors suspect that when the flow is non-turbulent, the instantaneous streamline patterns for each part of the vortex-shedding cycle will have the same qualitative features as the fully turbulent phase-averaged results. Some evidence for this is given in the present paper (see §2).

Instantaneous streamline patterns have often been ignored in unsteady-flow studies and streaklines have been used more often. The relationship between instantaneous streamlines and streaklines is extremely complex. Streaklines can be used to give an idea of where the vorticity resides in a flow field, but tell us very little about the surrounding flow field and the entrainment processes. Instantaneous streamline patterns can be obtained photographically from short-time exposures of small particles such as aluminium which have been introduced into the flow. The motions of these particles give a field of short streaklines. It can be shown that over very short time intervals, streaklines, pathlines and instantaneous streamlines are identical. See for example Kline (1965).

Of course, the above idea of obtaining instantaneous streamline patterns is not new. In fact, Nayler & Frazer (1917) attempted this technique when investigating the vortex shedding behind a circular cylinder in a water channel. By introducing neutrally buoyant oil droplets (a mixture of carbon tetrachloride & xylene) into the water, and by recording the motion of the droplets on a ciné film, Nayler & Frazer

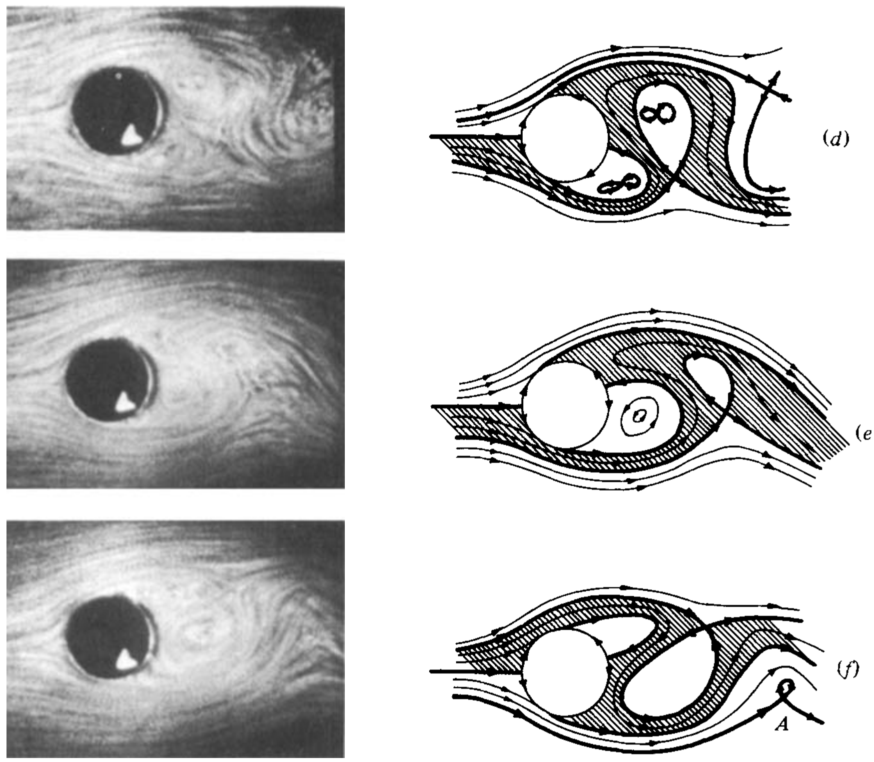

FIGURE 1. Flow in the near wake of a cylinder starting from rest. Observer moving with cylinder. Each picture obtained by exposing 40 consecutive frames from Prandtl's movie. Authors' interpretations also shown. Sequence of events begins at (*a*) and continues to (*f*). Non-dimensional time increment $(U_\infty \Delta t)/D \simeq 0\cdot3$ between each picture, where U_∞ is the free-stream velocity and D is the diameter of the cylinder. Cross-hatchings indicate instantaneous alleyways.

were able to obtain a series of instantaneous streamline patterns at different parts of the vortex shedding cycle. However, their interpretation of the pattern violated some of the geometrical properties of critical points (see Perry & Fairlie 1974).

The main objective of the present paper is therefore to examine the properties of the instantaneous streamline and streakline patterns behind a circular cylinder during the process of vortex shedding. To obtain instantaneous streamlines, the authors decided to use the technique described earlier. This was achieved by using the movie produced under the direction of Prandtl in the 1920s (see Shapiro & Bergman 1962). This movie was produced under constant illumination (i.e. no strobing was applied) and contained flow-visualization experiments conducted in a water channel on flow past bodies of various geometries with small aluminium particles suspended on the free surface.†

To obtain streakline patterns behind the cylinder, the present authors conducted the experiment in an open-circuit water channel using dye as an indicator. The cylinder used was spanned across the working section and was fully submerged in the water. The Reynolds number based on the diameter of the cylinder was of the order of 100.

† Over 200 frames of the movie corresponded to one vortex-shedding cycle.

2. An interpretation of Prandtl's movie using properties of critical points

Prandtl (see Shapiro & Bergman 1962) produced a movie of flow around bodies using aluminium particles on a free surface. Each frame of the movie was produced by an extremely short time exposure and no instantaneous streamlines can be seen. The authors therefore decided to expose 40 consecutive frames of the movie on one photographic plate. This process was repeated for various parts of the shedding cycle behind the bodies. In this way a series of instantaneous streamline pictures was obtained. Figure 1 shows the case for a cylinder starting from rest. Various salient features of the flow patterns become obvious. These are called critical points (i.e. points where the slopes of the instantaneous streamlines become indeterminate). These critical points have been classified by Perry & Fairlie (1974) but for the work described here, certain properties of these critical points and other flow pattern features are important. These properties are consequently summarized below.

(i) Viscous critical points are points of zero vorticity. These occur only on the boundary where the no slip condition applies. From the equations of Perry & Fairlie (1974), it can be shown that if we expand in a Taylor series about the critical point in both space and time, then to first order, the critical point has the same properties as a steady critical point, but translates with uniform velocity relative to the boundary. To see a viscous critical point, an observer must be stationary relative to the boundary. Relative to any other observer, the critical point disappears.

(ii) Inviscid critical points are singularities at the boundary where the no-slip condition has been relaxed. These can also be thought of as critical points within the fluid. Again, it can be shown from the equations of Perry & Fairlie (1974) that, to first order in a Taylor-series expansion about the critical point, all viscous terms cancel, even though the flow may be viscous elsewhere. For this reason, such critical points are referred to as inviscid critical points. Such a model is suitable for critical points away from boundaries. To first order in both space and time, inviscid critical points translate with uniform velocity equivalent to the velocity U_m of the pressure maxima or minima†. If an observer is moving with this velocity, then relative to him, the critical points are located at the pressure maxima or minima. Relative to any other observer, however, these critical points will be displaced from the pressure maxima or minima.

Using the pictures of figure 1, properties (i) and (ii), and the well-known fact that instantaneous streamlines, irrespective of whether they occur in steady or unsteady flow, must obey continuity, a simple model for the flow in the cavity is proposed for the steady-state oscillation. This proposed model is shown in figure 2. It should be pointed out that in two-dimensional incompressible flow the only critical points allowable are centres and saddles, otherwise continuity will be violated. Only the separatrices are shown.‡ As shown in figures 1 (*a*,*b*), the cavity which forms during the starting-up process is closed and all the saddles are joined together. This is the classical picture of cavity flow. However, during the vortex-shedding process (see

† In steady flow, pressure maxima and minima correspond with saddles and centres respectively.

‡ In critical-point terminology, a separatrix is a streamline which leaves or terminates at a saddle.

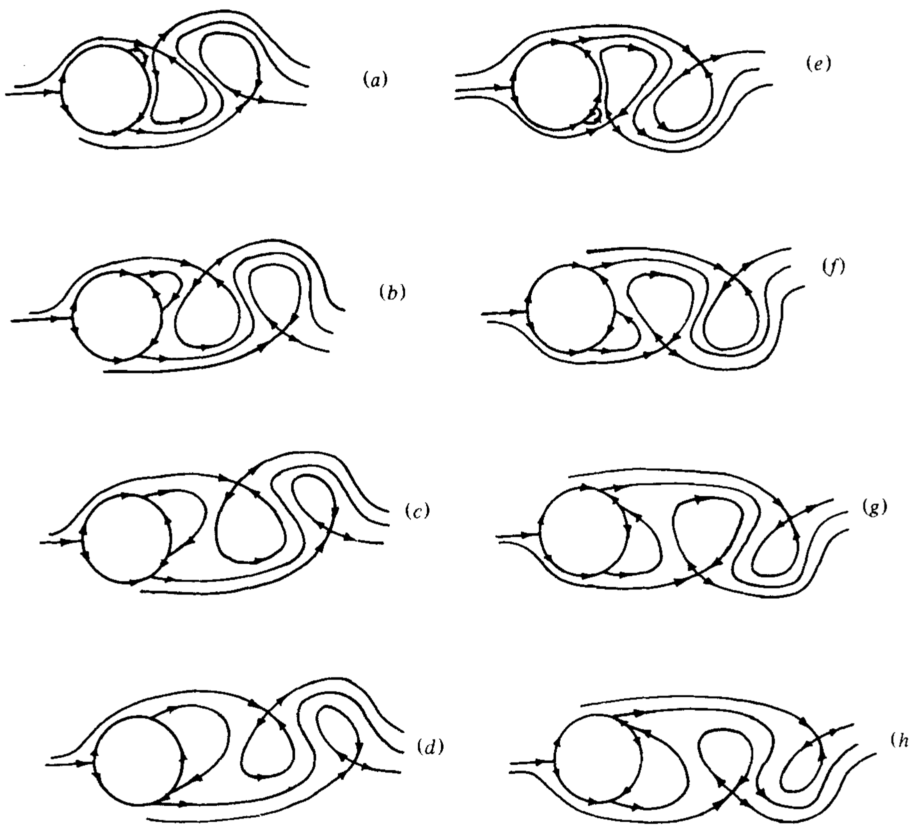

FIGURE 2. Proposed simple model for steady vortex shedding. Observer moving with the cylinder. Only separatrices shown. Sequence is from (*a*) to (*h*).

figures 1*c–f*), the cavity is open and the saddles are not necessarily joined by the separatrices, and instant 'alleyways' of fluid penetrate the cavity. These 'alleyways' are shown in figure 1 by the cross-hatching. The formation of 'alleyways' can also be seen in the computer plots of Fromm & Harlow (1963) and in the flow visualization of Taneda (1978), who also used the short-time exposure of aluminium particles to obtain streamline patterns behind bodies such as circular cylinders, elliptical cylinders and flat plates. Unfortunately, he presented his results without further interpretation.

Flow behind bodies of other geometries such as an elliptical cylinder or a bluff plate follow the same general model. However, in the case of the plate, the separation points on the body are fixed at the sharp edges. Figure 3 shows a typical instantaneous streamline pattern taken by Prandtl for the flow behind an elliptical cylinder at a Reynolds number (based on the major axis) of 250. This streamline pattern possesses the same general feature as that shown in figure 1 (*d*) for a cylinder.

Smits (1980) in conjunction with the present authors also performed a series of visual studies of the flow behind a two-dimensional bluff plate with sharp edges at a Reynolds number of the order of 3400. The plate had an aspect ratio of 1·76 but spanned across the width of the tunnel. Figure 4 (*a*) shows a typical streakline (i.e. smoke) pattern. Although these are streaklines, and the flow is turbulent with

FIGURE 3. Instantaneous streamlines behind an elliptical cylinder. Reynolds number based on the major axis = 250 (from Prandtl & Tietjens (1934), figure 66).

(a)

Caption for figure 4 (a) on p. 83.

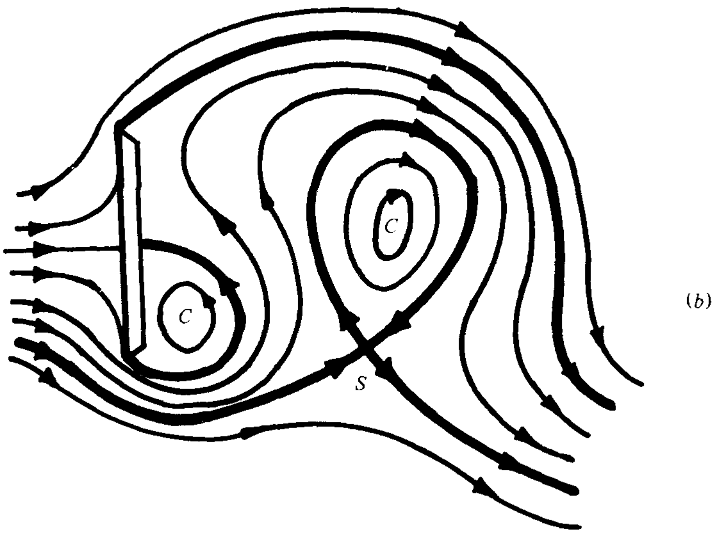

FIGURE 4. (*a*) Typical smoke pattern in the wake of a two-dimensional bluff plate. Reynolds number = 3400. Aspect ratio of the plate = 1·76, but spanned the width of the tunnel. (*b*) Instantaneous streamline pattern corresponding to (*a*). Sepatrices are shown. *S*, saddle; *C*, centre.

associated three dimensionality, individual clumps of smoke have smeared out in the time exposure, giving a picture resembling the instantaneous streamline pattern in figure 4(*b*). At this higher Reynolds number, the basic mechanism of vortex shedding appears to be very similar to that of the low-Reynolds-number case shown in figure 3. Based on this result, and the results of Cantwell (1975), the authors believe that the proposed model given in figure 2 is valid irrespective of the Reynolds number. Of course, for high-Reynolds-number cases, the experimental data have to be sampled conditionally on the basis of phase.

In all the cases considered so far (figures 1–4) the observer is stationary relative to the body. Therefore, critical points on the surface appear as critical points (property (i)). Also, since the flow immediately behind the body is inactive (i.e. the velocity is low), the critical points within the fluid are approximately in their correct positions (by property (ii)). However, further downstream (2 or 3 wavelengths), the eddies accelerate rapidly until they reach their final convection velocity. When this happens the centres and saddles are displaced from their correct positions (property (ii)). To a stationary observer, the centres and saddles will merge to approach 'centre saddles' where the separatrices join at an apex (point *A* in figure 1*f*). To see these critical points as steady, the observer must move with the convection velocity of the pressure maxima and minima, U_m.

3. Properties of the far wake in relation to different moving observers

The different streamline patterns as seen by different moving observers can also be illustrated if we use von Kármán's (1912) stable vortex spacing (see also Milne-Thomson 1968; Lamb 1945) to solve for the complex potential with the effect of the velocity of the observer included. The generated stream functions relative to different

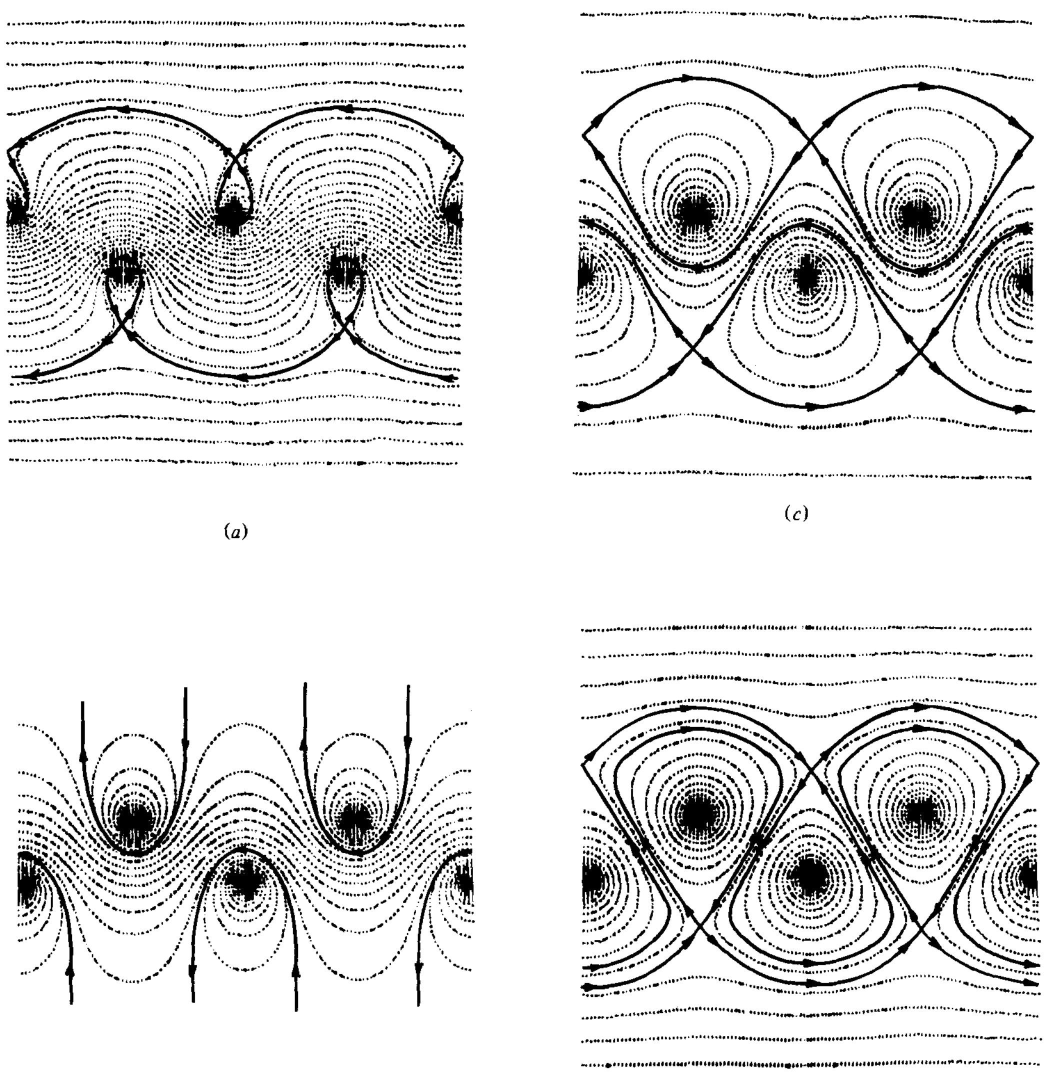

(a) (c)

(b) (d)

Caption for figures 5 (a–d) on facing page.

observers are shown in figure 5. In figure 5(a), the observer is moving faster than the free stream and faster than the eddies. Note that the saddles of the top eddies are above the eddies and are joined at the top. In figure 5(b), the observer is moving with the free stream and faster than the eddies. The saddles for this case are at infinity. Goldstein (1965) erroneously reported that the pattern of figure 5(b) corresponds to the observer moving with the eddies. This error has been repeated in many textbooks. The figure caption explains various other cases shown. It should be noted that the centres (or vortices) do not move laterally – only the saddles do this. This is because the centres here are irregular; i.e. they are point vortices which possess infinite tangential velocity at their origins. Hence the motion of the observer

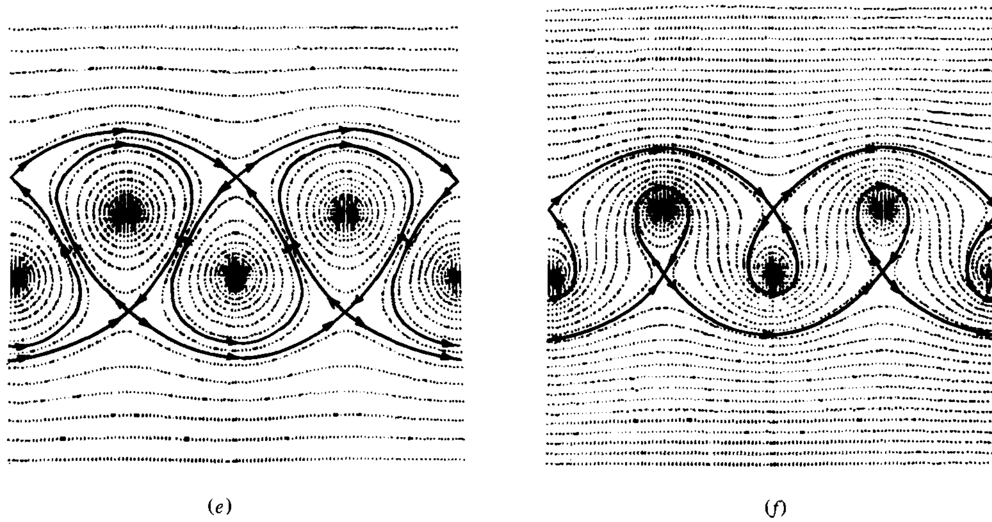

FIGURE 5. Kármán vortex street as seen by different observers. Let $-V_E$ be the velocity of eddies relative to free stream. V_E is a positive number and positive velocity is from left to right. (*a*) Observer moving at $1{\cdot}0\ V_E$ i.e. observer is moving faster than free stream and faster than eddies. (*b*) Observer moving at $0\ V_E$, i.e. observer is moving with the free stream but faster than the eddies. (*c*) Observer moving at $-0{\cdot}4\ V_E$, i.e. observer is moving slower than free stream but faster than the eddies. (*d*) Observer moving at $-0{\cdot}8\ V_E$, i.e. observer is moving slower than free stream but faster than the eddies. This happens to give almost-connected separatrices. (*e*) Observer moving at $-1{\cdot}0\ V_E$, i.e. observer is moving slower than free stream but moving with the eddies. (*f*) Observer moving at $-2{\cdot}0\ V_E$, i.e. observer is moving slower than free stream and slower than the eddies.

has no effect on their location but their shape is altered. The centres discussed by Perry & Fairlie (1974) are regular with finite vorticity.

Figure 6(*a*) shows the smoke pattern of a Kármán vortex street taken by Zdravkovich (1969) who introduced smoke close to the stagnation point of a cylinder. In incompressible flow, vorticity is generated only at solid boundaries and this vorticity resides with the fluid (see Lighthill 1963; Batchelor 1967). Hence dye or smoke in the form of streaklines which originate from the surface must indicate the position of vortex sheets. Of course, it should be noted that at low Reynolds number, vorticity diffuses considerably more rapidly than does dye or smoke. Thus vortex sheets will be much thicker than indicated by the dye traces. However, the dye will indicate the position of the sheets. In figure 6 (*a*), one can see that this smoke has aligned itself with the separatrices of the steady streamline pattern as given in figure 5(*e*). It can also be seen that the smoke separatrices are approximately orthogonal at the saddles, hence they show that the flow is irrotational near the saddles. This can be deduced from the equations derived by Perry & Fairlie (1974) and also Perry, Lim & Chong (1980).

It can be seen from figure 6(*a*) that one of the separatrices is missing at each of the saddle points. This is a consequence of the way the sheets of smoke are folded in the shedding process and is elaborated upon in §4.

The Kármán vortex street can be observed to occur in a variety of situations besides two-dimensional wake-flow. The authors produced a Kármán vortex 'jet' from an oscillating tube with a rectangular outlet of high aspect ratio (see figure 6*b*).

(a)

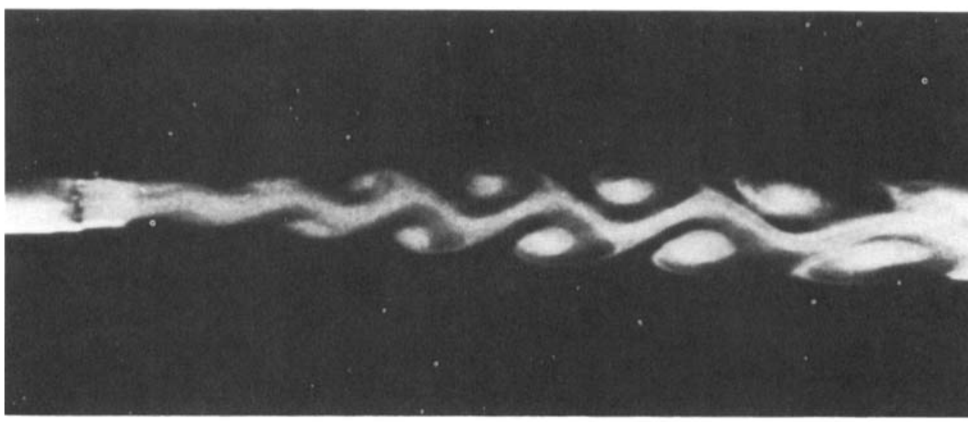

(b)

FIGURE 6. (a) Kármán vortex street behind a circular cylinder. Reynolds number based on the diameter $\simeq$ 50 (from Zdravkovich 1969). (b) Kármán-vortex-jet structure. Reynolds number based on the smallest side of the rectangular tube exit $\simeq$ 90. Tube outlet is recognizable on the left of the figure.

The tube was oscillated in a sinusoidal mode using the technique of Perry & Lim (1978). Note that the eddies in figure 6(b) are pointing in the opposite direction to that shown in figure 6(a) for a cylinder.

4. Dye experiments

The authors also carried out some experiments in a water tunnel with a circular cylinder set across the working section. Positive and negative vorticity were coloured blue and red respectively. This was done by introducing blue dye on the upper surface of the cylinder at an angular position of approximately 80° from the front stagnation point. Similarly red dye was introduced on the lower surface. The cylinder was completely submerged in the water tunnel. Figure 7 (plate 1) shows such dye traces in a Kármán vortex street behind the cylinder. Generally, the indentations which form on the vortex sheet correspond with instantaneous alleyways. However, centres did not necessarily correspond with the roll-up of the vortex sheet, partly because the flow is unsteady and partly because many layers of dye and hence

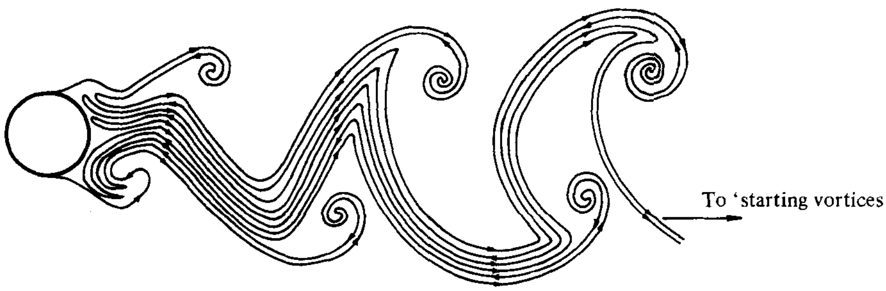

FIGURE 8. Schematic 'threading diagram' of vortex sheet in a Kármán vortex street. The progressive folding of the sheet can be traced by following the arrows.

vorticity are convected into the cavity, allowing centres to form within the cavity. Figure 7 shows these layers.

It is well known that a streakline (dye in this case) can never be broken. It represents a flexible barrier which fluid can never cross, even though, in the actual flow situation, it may be stretched and become so highly convoluted that the original vortex sheet may become unrecognizable as a continuous sheet. In the present situation, the fluid entering the cavity via the alleyways is bounded on one side by the dye interface. On the next cycle the same applies to the next 'body' of fluid. As a result, the various 'bodies' of fluid within the cavity are recognizable and separated from each other by a dye interface. These 'bodies' of fluid form a queue and are successively stacked up one behind the other and then move in jumps towards the solid body, awaiting their turn to be 'squeezed' out of the cavity and carried away by a Kelvin–Helmholtz-like roll-up. Figure 8 presents a schematic 'threading' diagram proposed by the present authors for this 'multiple-folding' process and shows that every eddy produced is ultimately interconnected with every other eddy. The two sets of vortex sheets intertwine with each other in the far wake. This ultimately forms a pattern as shown in figure 6(*a*). However, in this figure the individual layers of dye (or smoke) have been smeared out by diffusion. Gerrard (1978) also observed this 'multiple-folding' phenomenon and referred to it as 'fingers'. At Reynolds numbers beyond 140, he observed that these 'fingers' are sometimes absorbed into the vortices of opposing sign at the opposite side of the wake. The authors did not observe this at Reynolds number of 80† and the 'threading diagram' shown in figure 8 would be modified at higher Reynolds numbers. Nevertheless, the authors contend that the broad features of the instantaneous streamline patterns do not alter with Reynolds number (i.e. the model given in figure 2 is still applicable). Also Gerrard did not relate this 'multiple-folding' phenomenon to instantaneous streamline patterns.

To establish a relationship between dye traces and instantaneous streamline patterns, the authors introduced aluminium particles into the flow and illuminated them with a sheet of laser light. Figure 9(*a*) shows the resulting instantaneous streamlines together with dye, and figure 9(*b*) shows the authors' interpretation. As mentioned earlier, the centres which form in the cavity do not necessarily correspond with the roll-up of the vortex sheet. This is partly because of the vorticity

† When this absorption did occur, it could always be attributed to buoyancy of the dye; e.g. see figure 7(*b*).

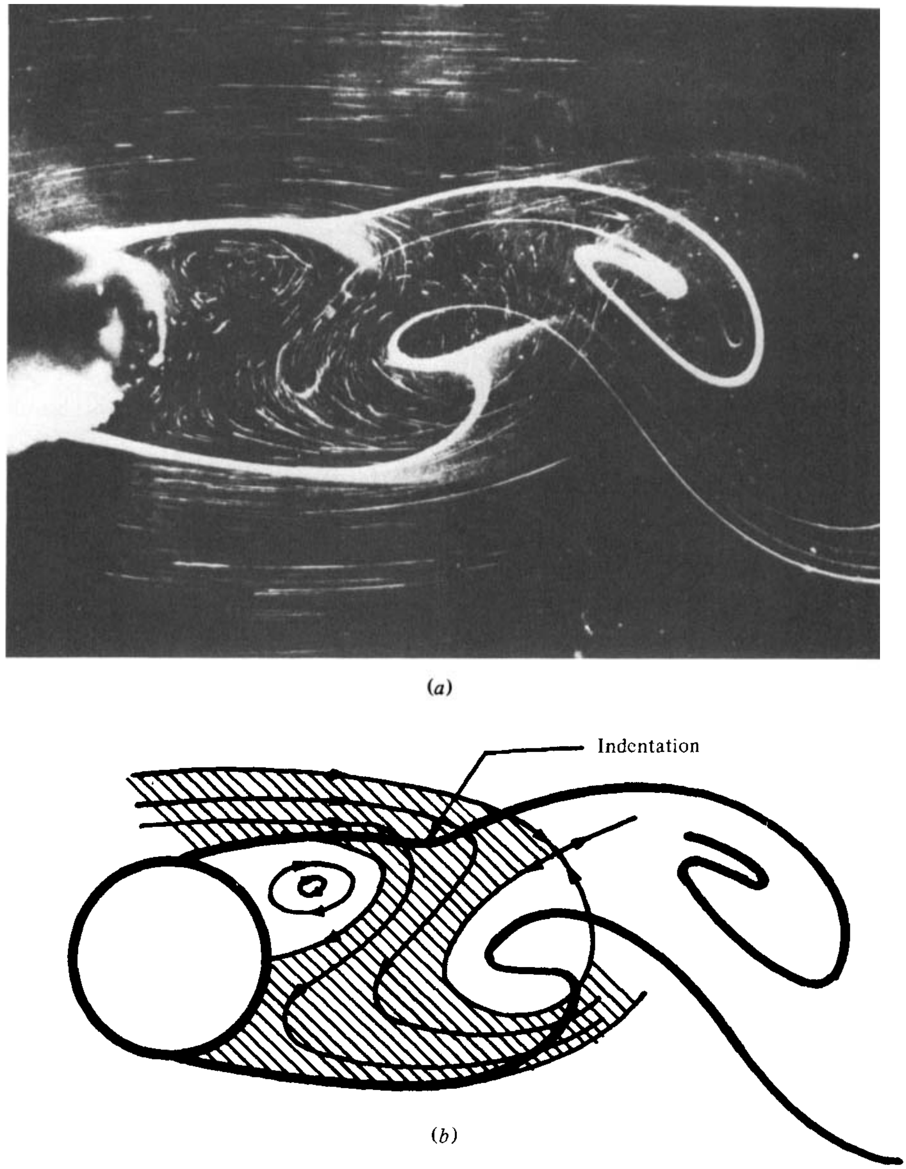

FIGURE 9. (*a*) Instantaneous streamlines and dye traces (streaklines or vortex sheet) behind circular cylinder. Reynolds number is of the order of 100. (*b*) Author's interpretation of (*a*). Cross-hatching indicates instantaneous alleyway.

being convected into the cavity through multiple folding of the vortex sheet as shown in figure 8. Also, from such studies the authors conclude that the initial indentations in the dye correspond to the instantaneous alleyways.

5. Discussion and conclusion

It can be seen that the unsteady cavity behind a vortex-shedding cylinder is complex. Rather than a stagnant 'pool' of fluid, the cavity should be thought of as a region where vortex sheets are undergoing a multiple-folding process and where each vortex shed is always ultimately connected back to the cavity by its own 'umbilical cord' or 'thread'. This explains how vorticity is convected into the cavity. Viscous diffusion, although present, is not the basic mechanism. This would explain why the pattern is insensitive to Reynolds number.

From the movie which Prandtl made on flow around bodies, a sequence of instantaneous streamline patterns of the flow behind a circular cylinder was obtained. Interpretation of these streamline patterns at different stages of vortex shedding show that the classical picture of a closed cavity behind a body is true only in the time-averaged sense. However, the cavity is closed during the starting-up-process. Once vortex shedding begins, instantaneous 'alleyways' of fluid penetrate the cavity.

Properties of the far wake have also been identified. If one moves at the correct convection velocity the pattern becomes steady and the instantaneous streamline pattern corresponds to the streakline pattern. Given a sufficient time of development, the streakline pattern will align itself with the separatrices of the streamline pattern.

The authors wish to acknowledge the financial assistance of the Australian Research Grants Committee, the National Energy Research, Development and Demonstration Council, and the Australian Institute of Nuclear Science and Engineering.

REFERENCES

BATCHELOR, G. K. 1967 *An Introduction to Fluid Dynamics*. Cambridge University Press.

BEARMAN, P. W. & GRAHAM, J. M. R. 1980 Vortex shedding from bluff bodies in oscillatory flow: A report on Euromech 119. *J. Fluid Mech.*, **99**, 225.

BERGER, E. & WILLE, R. 1972 Periodic flow phenomena. *Ann. Rev. Fluid Mech.* **4**, 313.

CANTWELL, B. J. 1975 A flying hot wire study of the turbulent near wake of a circular cylinder at a Reynolds number of 140000. Ph.D. thesis, California Institute of Technology.

FROMM, J. E. & HARLOW, F. H. 1963 Numerical solution of the problem of vortex sheet development. *Phys. Fluids* **6**, 975.

GERRARD, J. H. 1978. The wakes of cylindrical bluff bodies at low Reynolds number. *Phil. Trans. R. Soc. Lond.* A **289**, 351.

GOLDSTEIN, S. 1965 *Modern Developments in Fluid Dynamics*, vol. 1. Dover.

VON KÁRMÁN, T. 1912 *Collected works*, vol. 1 (1902–1913), p. 339. Butterworths.

KLINE, S. J. 1965 FM-48 Film loop. National Committee for Fluid Mechanics Films.

LAMB, H. 1945 *Hydrodynamics*, 6th edn. Dover.

LIGHTHILL, M. J. 1963 In *Laminar Boundary Layers* (ed. L. Rosenhead), pp. 48–88. Clarendon Press.

MAIR, W. A. & MAULL, D. J. 1971 Bluff bodies and vortex shedding – a report on Euromech 17. *J. Fluid Mech.* **45**, 209.

MILNE-THOMSON, L. M. 1968 *Theoretical Hydrodynamics*, 5th edn. Macmillan.

MORKOVIN, M. V. 1964 Flow around circular cylinder – kaleidoscope of challenging fluid. phenomena. In *Proc. A.S.M.E. Symp. on Fully Separated Flows, Philadelphia*, pp 102–118. A.S.M.E.

NAYLER, J. L. & FRAZER, R. A. 1917 Vortex motion. (i) Preliminary report upon an experimental method of investigating, by aid of kinematograph photography, the history of eddying flow past a model immersed in water. *Reports and Memoranda* (*new series*), no. 332. *Tech. Rep. of the Adv. Committee for Aeronautics.*

PERRY, A. E. & FAIRLIE, B. D. 1974 Critical points in flow patterns. *Adv. Geophys.* B **18**, 299.

PERRY, A. E. & LIM, T. T. 1978 Coherent structure in coflowing jets and wakes. *J. Fluid Mech.* **88**, 451.

PERRY, A. E., LIM, T. T. & CHONG, M. S. 1980 The instantaneous velocity fields of coherent structures in coflowing jets and wakes. *J. Fluid Mech.* **101**, 243.

PERRY, A. E. & WATMUFF, J. H. 1981 The phase-averaged large-scale structures in three-dimensional turbulent wakes. *J. Fluid Mech.* **103**, 33.

POPHAM, A. E. 1946 *The Drawings of Leonardo de Vinci.* Jonathan Cape.

PRANDTL, L. & TIETJENS, O. G. 1934 *Applied Hydro- and Aeromechanics.* Dover.

SHAPIRO, A. H. & BERGMAN, R. 1962 Experiments performed under the direction of L. Prandtl (Göttingen). FM-11 Film loop. National Committee for Fluid Mechanics.

SMITS, A. J. 1980 A visual study of separation bubbles. *Int. Symp. on Flow Visualization, Bochum.* Hemisphere.

TANEDA, S. 1978 Visual study of unsteady separated flows and bodies. *Prog. Aero. Sci.* **17**, 287.

WILLE, R. 1960 Karman vortex streets. *Adv. Appl. Mech.* **6**, 273.

WILLE, R. 1966 On unsteady flows and transient motions. *Prog. Aero. Sci.* **7**, 195.

ZDRAKOVICH, M. M. 1969 Smoke observations of the formation of a 'Kármán' vortex street. *J. Fluid Mech.* **37**, 491.

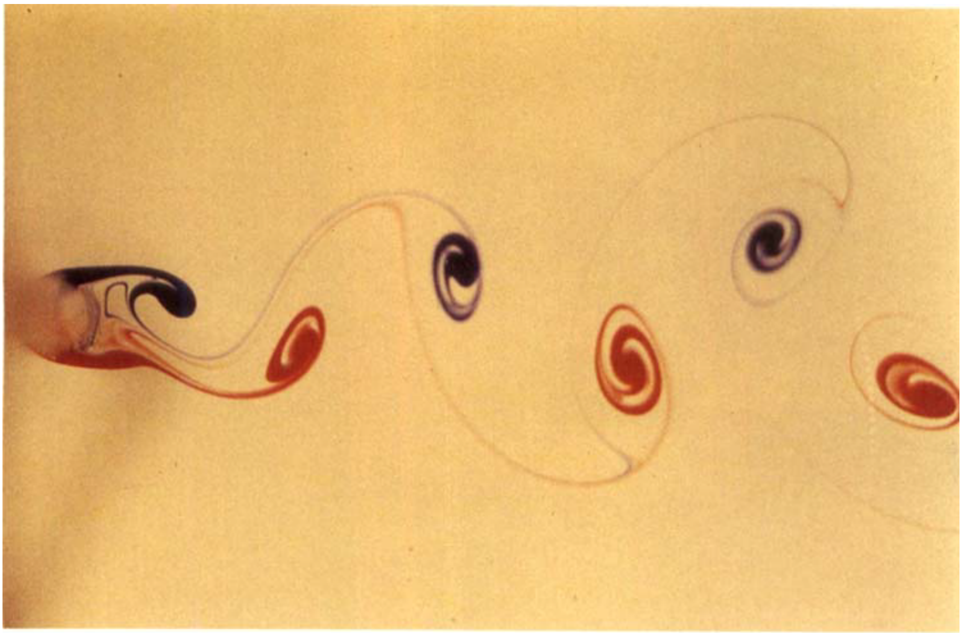

(*a*)

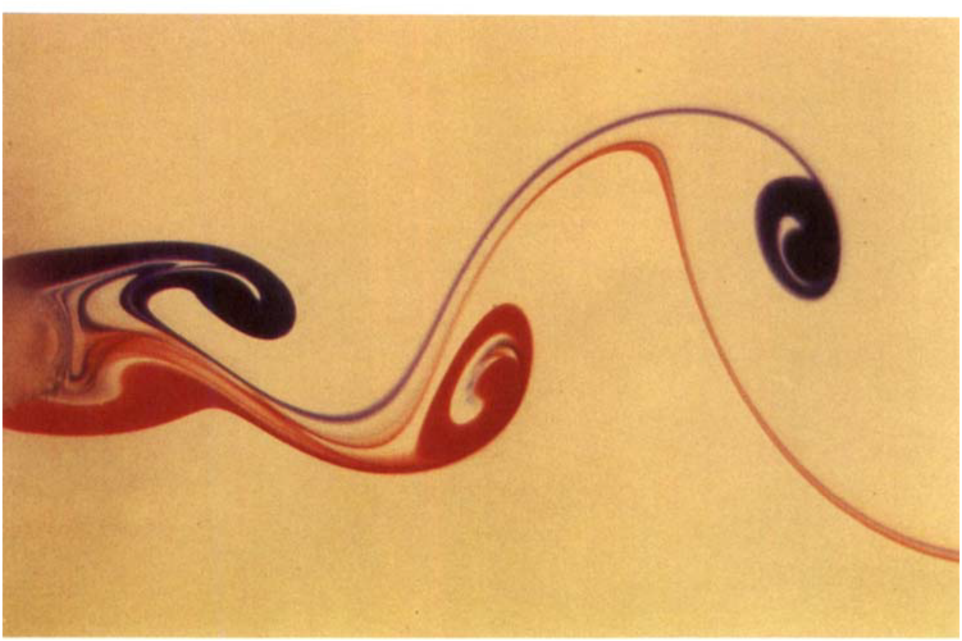

(*b*)

FIGURE 7. (*a*) Typical dye traces in a Karman vortex street behind a circular cylinder. (*b*) Close-up view of Karman vortex street near the cylinder. Blue dye corresponds to positive vorticity and red dye corresponds to negative vorticity. Reynolds number (based on the diameter of the cylinder) = 80. Blue dye at the bottom is due to buoyancy.